Cytotoxic impact of a perillyl alcohol–temozolomide conjugate, NEO212, on cutaneous T-cell lymphoma *in vitro*

Catalina Silva-Hirschberg, Hannah Hartman, Samantha Stack, Steve Swenson, Radu O. Minea, Michael A. Davitz, Thomas C. Chen and Axel H. Schönthal [ID]

Abstract

Background: Mycosis fungoides (MF) and Sézary syndrome (SS) are subtypes of primary cutaneous lymphomas and represent complex diseases regarding their physiopathology and management. Depending on the stage of the disease, different treatment regimens are applied, but there is no consensus on an optimal approach. Prognosis for patients with early stage MF is favorable, but significantly worsens in advanced disease and in SS, where patients frequently relapse and require multiple therapies.

Methods: We investigated the potential anticancer effects of NEO212, a novel compound generated by covalently conjugating perillyl alcohol (a natural monoterpene) to temozolomide (an alkylating agent), on MF and SS cell lines *in vitro*. HUT-78, HUT-102, and MyLa cells were treated with NEO212 under different conditions, and drug effects on proliferation, viability, and apoptosis were characterized.

Results: NEO212 inhibited proliferation, diminished viability, and stimulated apoptosis in all cell lines, although with varying degrees of potency in the different cell lines. It down-regulated c-myc and cyclin D1 proteins, which are required for cell proliferation, but triggered endoplasmic reticulum stress and activation of caspases. Pretreatment of cells with antioxidants ascorbic acid and beta-mercaptoethanol prevented these NEO212-induced effects.

Conclusions: NEO212 exerted promising anticancer effects on SS and MF cell lines. The generation of reactive oxygen species (ROS) appears to play a key role in the NEO212-induced cell death process, because the blockage of ROS with antioxidants prevented caspase activation. We propose that NEO212 should be investigated further toward clinical testing in these tumor types.

Keywords: cutaneous T-cell lymphoma, mycosis fungoides, NEO212, perillyl alcohol, Sézary syndrome, temozolomide

Correspondence to:
Thomas C. Chen
Department of
Neurosurgery, Keck
School of Medicine,
University of Southern
California, 2011 Zonal
Avenue, Los Angeles, CA
90089, USA
tcchen@usc.edu

Axel H. Schönthal
Department of Molecular
Microbiology and
Immunology, Keck School
of Medicine, University of
Southern California, 2011
Zonal Avenue, HMR-405,
Los Angeles, CA 90089,
USA
schontha@usc.edu

Catalina Silva-Hirschberg
Hannah Hartman
Samantha Stack
Department of Molecular
Microbiology and
Immunology, Keck School
of Medicine, University of
Southern California, Los
Angeles, CA, USA

Steve Swenson
Radu O. Minea
Department of
Neurosurgery, Keck
School of Medicine,
University of Southern
California, Los Angeles,
CA, USA

Michael A. Davitz
Leason Ellis, One Barker
Avenue, Fifth Floor, White
Plains, New York, NY, USA

Introduction

Primary cutaneous lymphomas are a heterogeneous group of extranodal non-Hodgkin lymphomas. In contrast to nodal non-Hodgkin lymphomas, most of which are B-cell derived, approximately 75% of primary cutaneous lymphomas are T-cell derived.[1] Cutaneous T-cell lymphomas (CTCLs) are rare and they are characterized by the presence of malignant T lymphocytes in the skin.[2,3] They represent 3.9% of all non-Hodgkin lymphomas with an annual incidence of 6.4–9.6 cases per million people in the United States.[4–6] Mycosis fungoides (MF) is the most common CTCL, whereas Sézary syndrome (SS) is much rarer. They account for 2–3% of all lymphomas[7] and comprise approximately 53% of all cutaneous lymphomas.[4] MF has an annual incidence of 5.6 per million

persons[3] representing 50% of all CTCLs,[8] whereas SS has an annual incidence of 0.1–0.3 per million persons and represents 2.5% of all CTCLs.[9]

Clinical symptoms of CTCL vary by subtype. In MF, a primarily cutaneous variant, symptoms remain mostly localized to the skin and include variably affected flat patches, thin plaques, or tumors. In comparison, SS, a variant with a leukemic component, presents as a more aggressive phenotype, in which the skin is diffusely affected and there is greater involvement of the systemic circulation.[10] In fact, the presence of >1000 Sézary cells/mm^{3} in the circulation represents a key diagnostic criterion for SS. In both diseases, skin biopsies can reveal the characteristic Sézary cells (T cells with cerebriform nucleus) that are infiltrating the epidermis. Although SS can arise as a progression of pre-existing MF, it more typically arises *de novo* and is generally considered a separate disease, rather than a leukemic progression of MF.[11,12]

The etiology of MF and SS is still unknown. It is thought to include chronic antigenic stimulation through viral or bacterial exposure, environmental exposures, and altered microRNA (miRNA) expression.[2] A recent case series examined a subset of hypertensive MF patients using hydrochlorothiazide, speculating that this diuretic may be associated with antigen-driven T-cell lymphoproliferation and could serve as a trigger for MF. In addition, individual genetic features have also been implicated in the development of CTCL.[1] Furthermore, a variety of genetic aberrations have been identified in MF, such as mutations in the tumor suppressor p53 gene and loss of other tumor suppressor genes, such as CDKN2A and CDKN2B. In addition, MF can have chromosomal gains and losses, and the Janus kinase (JAK) signal transducer and activator of transcription (STAT) pathways can be deregulated in MF and in CTCLs in general.[1,2,13]

Treatment strategies range from an expectant policy in early stage disease to hematopoietic stem cell transplantation, going through retinoids, immunotherapy, and extracorporeal photochemotherapy, among others.[3] The National Comprehensive Cancer Network (NCCN) guidelines outline classic treatments for MF/SS as determined by stage of the disease, estimated skin tumor burden, presence of unfavorable prognostic factors, age, and other comorbidities, such as cardiovascular disease, dyslipidemia, low thyroid function, etc., that can affect quality of life.[14] Although there are several therapies recognized by the NCCN for the treatment of MF/SS, there is a paucity of effective therapies providing durable responses. Targeted therapies have variable response rates ranging from 30% to 67%, with complete responses no higher than 41%[15] because none of these approaches are curative and patients frequently have relapses necessitating ongoing treatments.[14] Even with extensive treatment, the prognosis of these diseases at their advanced stages remains poor. MF has a 27% 5-year survival in advanced disease,[2] which in SS decreases to a 15% 5-year survival.[7]

NEO212 is a novel experimental drug that has revealed striking therapeutic activity in a variety of preclinical cancer models, including glioblastoma (GBM), melanoma, nasopharyngeal carcinoma, and brain-metastatic breast cancer.[16–19] It is a chimeric molecule that was generated by covalent conjugation of perillyl alcohol (POH) to temozolomide (TMZ). POH, a monoterpene related to limonene, is a natural constituent of caraway, lavender oil, cherries, cranberries, celery seeds, and citrus fruit peel.[20] It showed significant anticancer activity in a number of preclinical studies.[21] However, when tested as an oral formulation in several phase I/II trials with cancer patients, it did not produce convincing therapeutic outcomes.[21] Although POH was abandoned as an oral agent, currently ongoing clinical studies with recurrent GBM patients are investigating whether an intranasal formulation of this compound might be more successful.[22]

TMZ is an alkylating agent approved for the treatment of newly diagnosed GBM and refractory anaplastic astrocytoma.[23] It is also occasionally used for metastatic melanoma and other cancers, but the response rate is low.[24] Although TMZ methylates several moieties in different bases of the DNA backbone, it is methylation of the O6-position of guanine (mO6G) that is the decisive toxic lesion that is responsible for triggering subsequent cell death. However, mO6G can be repaired by the DNA repair enzyme O6-methylguanine DNA methyltransferase (MGMT), which removes the methyl group set by TMZ, thereby preventing the cytotoxic sequelae of this lesion. As a result, tumors that express significant levels of MGMT are highly resistant to TMZ therapy.[25,26]

In our prior work, we studied the anticancer activity of NEO212 in preclinical models and discovered much increased cancer therapeutic potency *in vitro* and *in vivo*.[16–19] Although the underlying mechanisms for the enhancement of tumoricidal activity in the conjugated compound remains to be fully characterized, the promising results obtained so far support the evaluation of its potency and benefit in other difficult-to-treat tumor types. Owing to the urgent medical need presented by the lack of effective therapies for CTCL, we performed an *in vitro* study to investigate the effects of NEO212 in CTCL.

Material and methods

Pharmacological agents
NEO212 was kindly provided by NeOnc Technologies (Los Angeles, CA) and was dissolved in DMSO at 100 mM. TMZ was obtained from the pharmacy at the University of Southern California (USC) or was purchased from Sigma Aldrich (St. Louis, MO) and dissolved in DMSO (Santa Cruz Biotechnology, Dallas, TX) to a concentration of 50 mM. POH was purchased from Sigma-Aldrich and diluted in DMSO to 100 mM. In all cases of cell treatment, the final DMSO concentration in the culture medium never exceeded 1% and was much lower in most cases. Stock solutions of all drugs were stored at −20°C. Staurosporine (STSP) was purchased from Selleck Chemicals (Houston, TX), stored at 4°C protected from light, and dissolved in DMSO before use. Ascorbic acid (AA) and beta-mercaptoethanol (β-ME; Sigma Aldrich) were prepared fresh before use. Crystalline AA was dissolved in phosphate-buffered saline (PBS) to 25 mM; β-ME was diluted in medium to 25 mM. General 3% household hydrogen peroxide was purchased from CVS Pharmacy and diluted in PBS and medium immediately before its addition to cells.

Cell lines
Three different human CTLC cell lines were used. HUT78 cells were purchased from the American Tissue Culture Collection (ATCC; Manassas, VA); this line originated from a patient with SS. HUT-102 also was obtained from the ATCC; this line originated from a patient with MF. MyLa cells were kindly provided by Julie Lewis in the lab of Michael Girardi at Yale University;[27] this line originated from a patient with MF. HUT-78 cells were propagated in Iscove's Modified Dulbecco's Medium (IMDM; from VWR, Radnor, PA, or from ATCC) supplemented with 15% fetal bovine serum (FBS). HUT-102 and MyLa cells were propagated in RPMI medium supplemented with 10% FBS. Both media also contained 100 U/ml penicillin and 0.1 mg/ml streptomycin. Penicillin, streptomycin, and RPMI (prepared with raw materials from Cellgro/MediaTech, Manassas, VA) were provided by the Cell Culture Core lab of the USC/Norris Comprehensive Cancer Center. HUT-102 cells occasionally received 2 ng/ml interleukin-2 into their medium, although a clear growth benefit did not become apparent. Cells were kept in a humidified incubator at 37°C and a 5% CO_2 atmosphere. FBS was obtained from Omega Scientific (Tarzana, CA) and from X&Y Cell Culture (Kansas City, MO). HUT-78 and HUT-102 cells were passaged for less than 6 months after receipt, thus representing authenticated cells.

MTT assay
Methylthiazoletetrazolium (MTT) assays were performed as follows. Cells were seeded into 96-well plates in a volume of 50 μl per well at $3.0–5.0 \times 10^5$ cells/ml. An additional 50 μl of medium containing various concentrations of drug (or vehicle) was added and the cells were incubated for different lengths of time. This was followed by the addition of 10 μl thiazolyl-blue tetrazolium (i.e. MTT; Sigma Aldrich) from a stock solution of 5 mg/ml in PBS. Cells were returned to the incubator for 4 h. Thereafter, the reaction was stopped and the cells were lysed by the addition of 100 μl solubilization solution (10% sodium dodecyl sulfate in 0.01 M hydrochloric acid). The 96-well plate was left in the cell culture incubator over night for complete solubilization of the MTT crystals, and the optical density (OD) of each well was determined the next day in an enzyme-linked immunosorbent assay (ELISA) plate reader at 560 nm. The background value (OD of control wells containing medium without cells + MTT + solubilization solution) was subtracted from all measured values. In individual experiments, each treatment condition was set up in quadruplicate, and each experiment was repeated several times independently.

Cell proliferation analysis
Cell proliferation was assessed by counting cells over time. Independent cell cultures were exposed to different concentrations of NEO212. At

different times, aliquots of cells were removed, mixed with Trypan blue, and counted in a hemocytometer. Blue cells were considered dead, whereas unstained cells were counted as live cells.

Fluorescence-activated cell sorting analysis

Cells were seeded in 6-well tissue culture plates at 2×10^5 cells/ml, followed by drug treatment. After 72 h, cells were collected, washed twice with PBS, transferred to a microcentrifuge tube, and suspended in 200 µl of $1\times$ binding buffer solution, which was made fresh from $10\times$ binding buffer (0.2 µm sterile-filtered 0.1 M HEPES, pH 7.4; 1.4 M NaCl; 25 mM $CaCl_2$). Then $1 \times$ µl of a 1 mg/ml 7-amino-actinomycin D (7-AAD) solution (Thermo Fisher Scientific, Waltham, MA) was added. After 20 min of incubation on ice, cell fluorescence was analyzed on a FACSAria Flow Cytometer (Becton Dickinson Biosciences Ltd., Franklin Lakes, NJ).

Immunoblots

Total cell lysates were prepared by disrupting cells with radio-immunoprecipitation assay (RIPA) buffer[28] supplemented with 1 mm PMSF (phenylmethylsulfonyl fluoride, Sigma Aldrich) and Pierce protease inhibitor mini tablets (1 tablet/10 ml; Thermo Fisher Scientific). Protein concentrations were determined using the Pierce BCA protein assay reagent (Thermo Scientific), and 50 µg of total cell lysate from each sample was separated by denaturing polyacrylamide gel electrophoresis (PAGE). Trans-blot (BioRad, Hercules, CA) was used for semi-dry transfer to Immobilon-P PVDF membranes (MilliporeSigma, Burlington, MA).

We used the following primary antibodies. For the detection of cleaved caspase 3: monoclonal antibody (MAB10753) from MilliporeSigma or monoclonal antibody (SC-271028) from Santa Cruz Biotechnology, Inc. (Dallas, TX). For cleaved caspase 4, CHOP, and b-actin: monoclonal antibodies (SC-1229, SC-166682, and SC-47778, respectively) from Santa Cruz. For MGMT, c-myc, and cyclin D1: polyclonal antibodies #2739, #13987, and #2922, respectively, from Cell Signaling Technology (Danvers, MA). For PARP-1: SC-56196 from Santa Cruz (specific for the cleaved form) and #9542 from Cell Signaling Technology (Danvers, MA), recognizing full-length and cleaved PARP1. Horseradish peroxidase–antibody conjugates (i.e. secondary antibodies) were obtained from Jackson ImmunoResearch Laboratories Inc (West Grove, PA). All antibodies were used according to the suppliers' recommendations. For detection, SuperSignal West Pico PLUS Chemiluminescent Substrate was used (Thermo Scientific). Most immunoblots were repeated at least once to confirm the results.

Statistical analysis

All parametric data were analyzed using Prism software (GraphPad Software, San Diego, CA). Student's t tests were applied to calculate the significance values. A probability value (p) <0.05 was considered statistically significant.

Results

NEO212 inhibits growth of MF and SS cell lines

NEO212's potential to inhibit the growth of CTCL was investigated *in vitro* with the use of three established cell lines, HUT78, HUT102, and MyLa. We used two established assays: the standard MTT assay, which primarily indicates cellular metabolic activity and thus viability, and the Trypan blue assay, which directly establishes cell number and thus reveals the proliferative activity of cells.

HUT78 cells were exposed to increasing concentrations of NEO212, and MTT assay was performed after 24, 48, 72, and 96 h. As shown in Figure 1(a), there was a clear time-dependent and concentration-dependent decrease in cellular viability. The earliest effect could be seen at 24 h with a concentration as low as 3 µM and an IC50 (50% decrease in viability) at 8 µM. At 48 h, the inhibitory effect of NEO212 became more pronounced, with an IC50 slightly below 3 µM. Longer incubation times, 72 and 96 h, reduced the IC50 further, although only slightly, as compared with the effects of NEO212 at 48 h. We therefore chose 72 and 96 h as the time points for analysis of the other two cell lines. As shown in Figure 1(b), HUT102 cells were somewhat less sensitive to NEO212 as compared with HUT78 cells, with IC50s at 72 and 96 h of 9 and 3 µM, respectively. In comparison, MyLa cells clearly were the least-sensitive cells, with IC50s of about 130 and 85 µM at 72 and 96 h, respectively (Figure 1(c)).

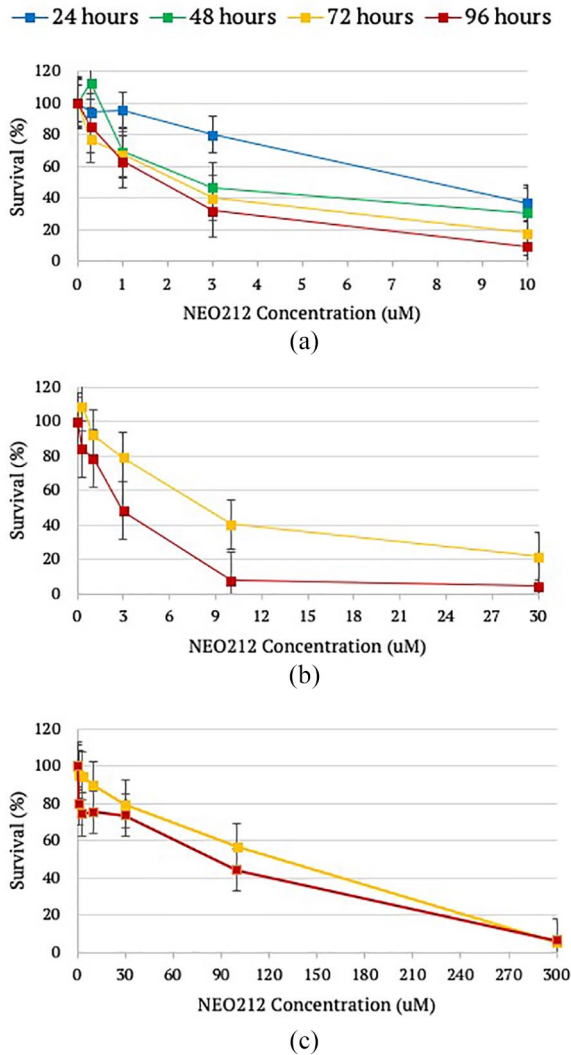The MTT results were complemented by counting the number of viable cells under different

Figure 1. NEO212 reduces cell viability.
Cells were exposed to increasing concentrations of NEO212, or vehicle only, or remained untreated. At different time points thereafter, standard methylthiazoletetrazolium (MTT) cell viability assay was performed: (a) HUT-78 cells; (b) HUT-102 cells; and (c) Myla cells. In all cases, viability of untreated cells was set to 100%. Vehicle-treated cells did not show differences to untreated cells.

Figure 2. NEO212 reduces cell proliferation.
Cells were exposed to increasing concentrations of NEO212 or remained untreated. At different time points thereafter, viable cells were counted *via* Trypan blue exclusion: (a) HUT-78 cells; (b) HUT-102 cells; and (c) Myla cells.
$^{*}p < 0.05$; $^{**}p < 0.01$ (as compared with untreated cells).

drug concentrations at different time points. Cells were treated with NEO212 at concentrations ranging from 1 to 300 μM, and viable cells (indicated by Trypan blue exclusion) were counted at 24, 48, 72, and 96 h. Intriguingly, the lowest concentration of NEO212 used, 1 μM, sufficed to exert proliferation-inhibitory effects in all three cell lines, with the strongest effect in HUT78 cells (Figure 2(a)), slightly less-pronounced activity in HUT102 cells (Figure 2(b)), and weaker activity in MyLa cells (Figure 2(c)). Higher concentrations of NE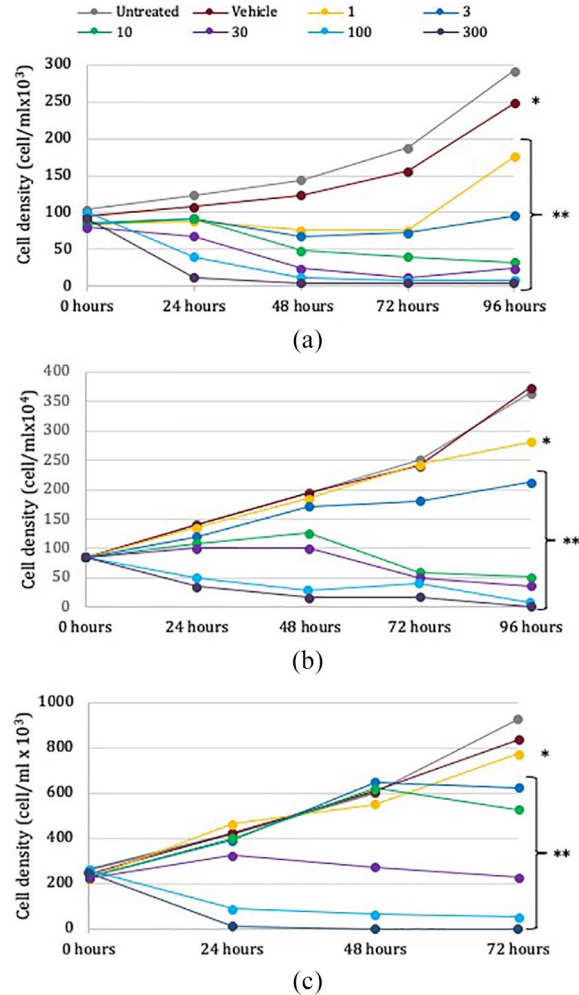O212 exerted correspondingly greater inhibitory activity in all three cell lines, and as before with the MTT assay, HUT78 cells displayed the greatest sensitivity, followed by HUT102 cells. In the case of HUT78 cells, we also noted that vehicle (DMSO) alone exerted minor inhibitory effect. However, this could only be observed at the highest DMSO concentration of 0.3%, which was that contained in the 300 μM NEO212 dose. Lower concentrations of DMSO did not exert such inhibitory effect, nor was this effect seen in the MTT assays.

Combined, the data from the above MTT and Trypan blue assays show that NEO212 inhibited proliferation and decreased viability in all three CTCL cell lines, although with varying potency.
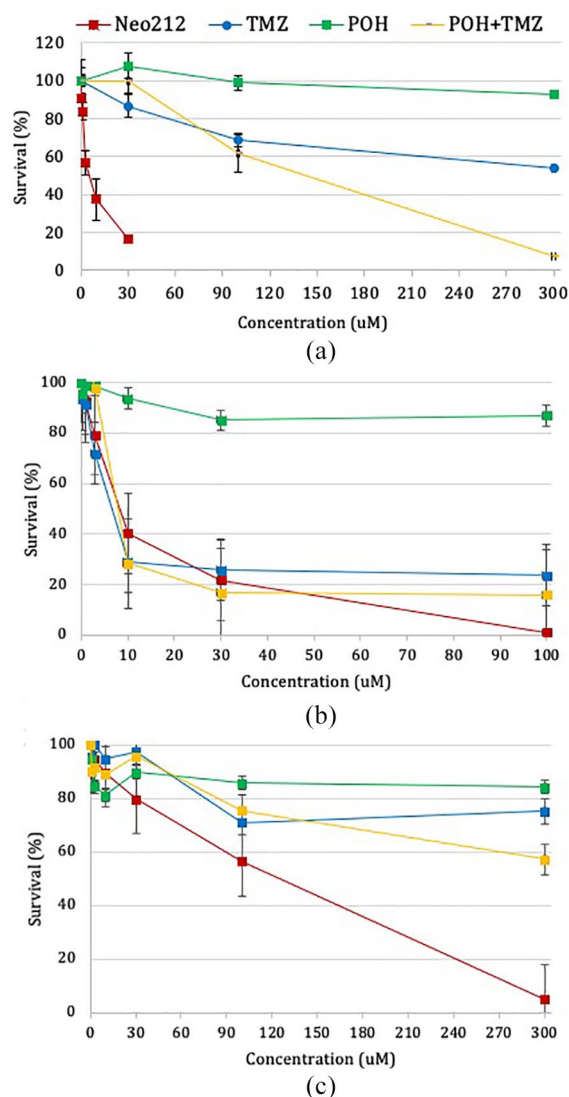
Figure 3. NEO212 is more cytotoxic than its individual constituents.
Cells were exposed to increasing concentrations of NEO212, temozolomide (TMZ), perillyl alcohol (POH), or TMZ in combination with POH (TMZ + POH). After 72 h, standard methylthiazoletetrazolium (MTT) cell viability assay was performed: (a) HUT-78 cells; (b) HUT-102 cells; and (c) Myla cells. In all cases, viability of untreated cells was set to 100%. Vehicle-treated cells did not show differences to untreated cells. The average (*n* = 4) ± standard deviation is shown.

Drug effects on proliferation were generally stronger and highly significant ($p < 0.01$). Although MyLa cells appeared more resistant to NEO212 in MTT assays, the Trypan blue exclusion assay revealed a delayed response of these cells to the drug, suggesting that NEO212 might require more time to unfold its inhibitory effect in these cells and trigger their demise.

NEO212 is more potent than the sum of its parts in HUT78 and Myla cells

As NEO212 is a chimeric molecule that was generated by covalent conjugation of two anticancer agents, POH and TMZ, we next compared its activity side by side with that of its two constituents, either individually or combined. Cells were treated with increasing concentrations of NEO212, POH alone, TMZ alone, or POH mixed with TMZ, and cell viability was determined by MTT assay after 72 h. As displayed in Figure 3(a), HUT78 displayed strikingly differential responses to these treatments. As before, NEO212 decreased viability very potently, with an IC50 of about 4 µM. In striking contrast, neither POH nor TMZ reached IC50 at concentrations up to 300 µM, and the combination of POH + TMZ had an IC50 of about 150 µM (i.e. 150 µM POH mixed with 150 µM TMZ).

In HUT102 cells, TMZ alone, as well as the mix of POH + TMZ, yielded similarly potent effects as NEO212 (all in the range of 6–8 µM IC50), whereas POH alone showed very minimal activity (Figure 3(b)). In MyLa cells, the IC50 of NEO212 was about 130 µM, whereas none of the other treatments reached IC50 at concentrations up to 300 µM (Figure 3(c)). In summary, this analysis revealed that responses in HUT78 and MyLa cells were similar, in that NEO212 was the most potent treatment (although at different IC50 values), whereas all others, including the combination of POH + TMZ, were unable to mimic the potency of NEO212. HUT102 cells, however, did not repeat this pattern; rather, these cells displayed similar sensitivity to NEO212, TMZ, and the POH + TMZ combination.

To gain some initial insight as to why HUT102 cells displayed greater sensitivity to TMZ as compared with HUT78 and MyLa cells, we used Western blot analysis to investigate the expression level of MGMT, a DNA repair protein known to confer strong resistance to TMZ.[25,26] In parallel, we included two established GBM cell lines (TMZ-resistant T98G and TMZ-sensitive U251) as positive and negative controls, respectively. As shown in Figure 4, HUT78 and MyLa cells presented with prominent MGMT expression similar to T98G cells, whereas HUT102 cells were negative for MGMT, as were U251 cells. Thus, the differential MGMT expression level in the three CTCL cell lines was aligned with their sensitivity to TMZ, but it did not correlate with these cells' sensitivity to NEO212.
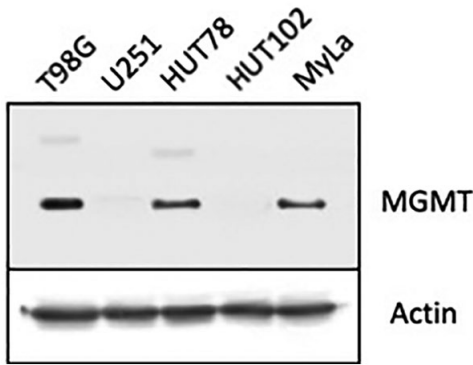
Figure 4. Differential expression of O6-methylguanine DNA methyltransferase (MGMT) protein in mycosis fungoides (MF) and Sézary syndrome (SS) cells.
Total cell lysates were subjected to Western blot analysis for MGMT expression. For comparison purposes, lysates from two glioblastoma cell lines, U251 (MGMT-negative) and T98G (MGMT-positive) were included. Actin was used as a loading control.

NEO212 causes apoptotic cell death

To further characterize the inhibitory effect of NEO212 on CTCL cells, especially in comparison with TMZ, we analyzed drug-induced cell death by fluorescence-activated cell sorting (FACS) analysis with 7-amino-actinomycin D (7-AAD) as a cell death marker. HUT78 cells were treated with 1, 3, 10, or 30 μM NEO212 or with 10, 30, 100, or 300 μM TMZ for 72 h. As a positive control, cells were also treated with staurosporine (STSP), a well-established inducer of apoptotic cell death.[29] As displayed in Figure 5, both NEO212 and TMZ triggered cell death, but NEO212 was substantially more potent. For instance, cell cultures treated with only 1 μM NEO212 showed 33% cell death, whereas the highest concentration of TMZ used, 300 μM, resulted in only 26% cell death. Increasing NEO212 concentrations to 30 μM resulted in 50% cell death, confirming its cell killing potency.
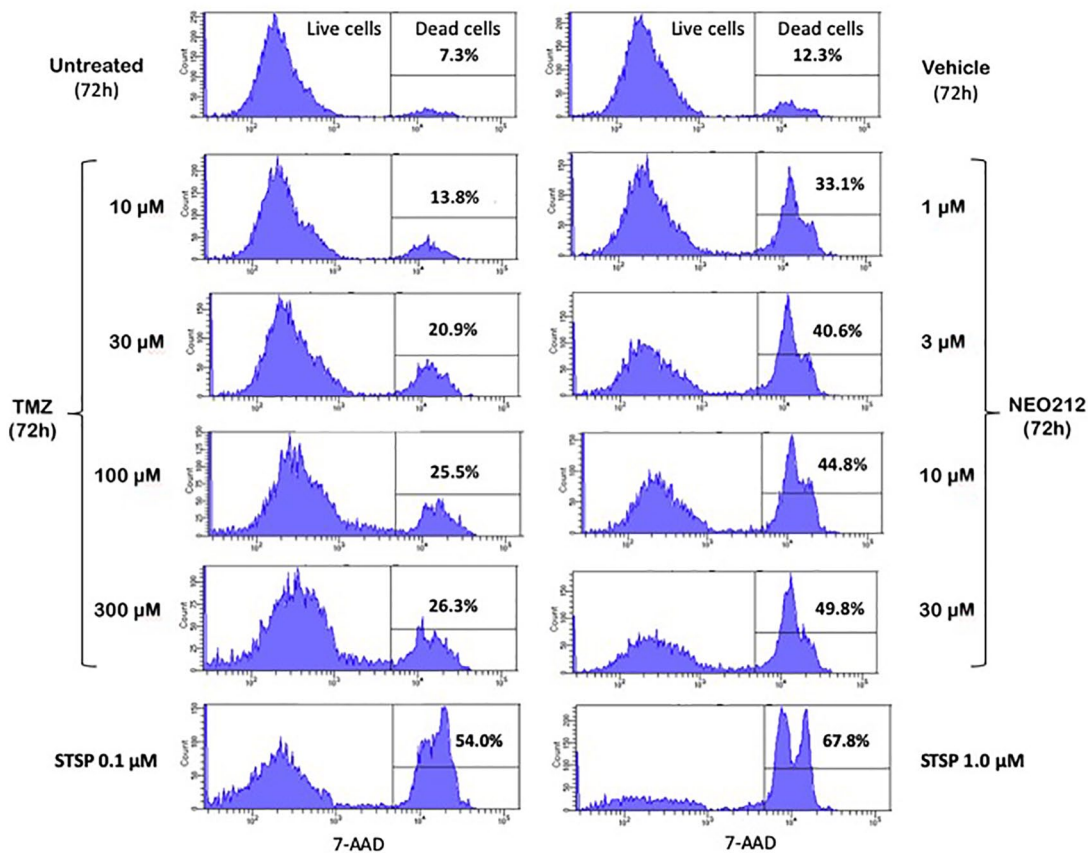

Figure 5. NEO212 triggers cell death more potently than temozolomide (TMZ).
HUT-78 cells were exposed to increasing concentrations of NEO212 or TMZ for 72 h. As a positive control, some cells received staurosporine (STSP) for 24 h. Thereafter, cells were stained with 7-AAD and subjected to fluorescence-activated cell sorting (FACS). Note that the lowest concentration of NEO212 (1 μM) was more potent than the highest concentration of TMZ (300 μM).
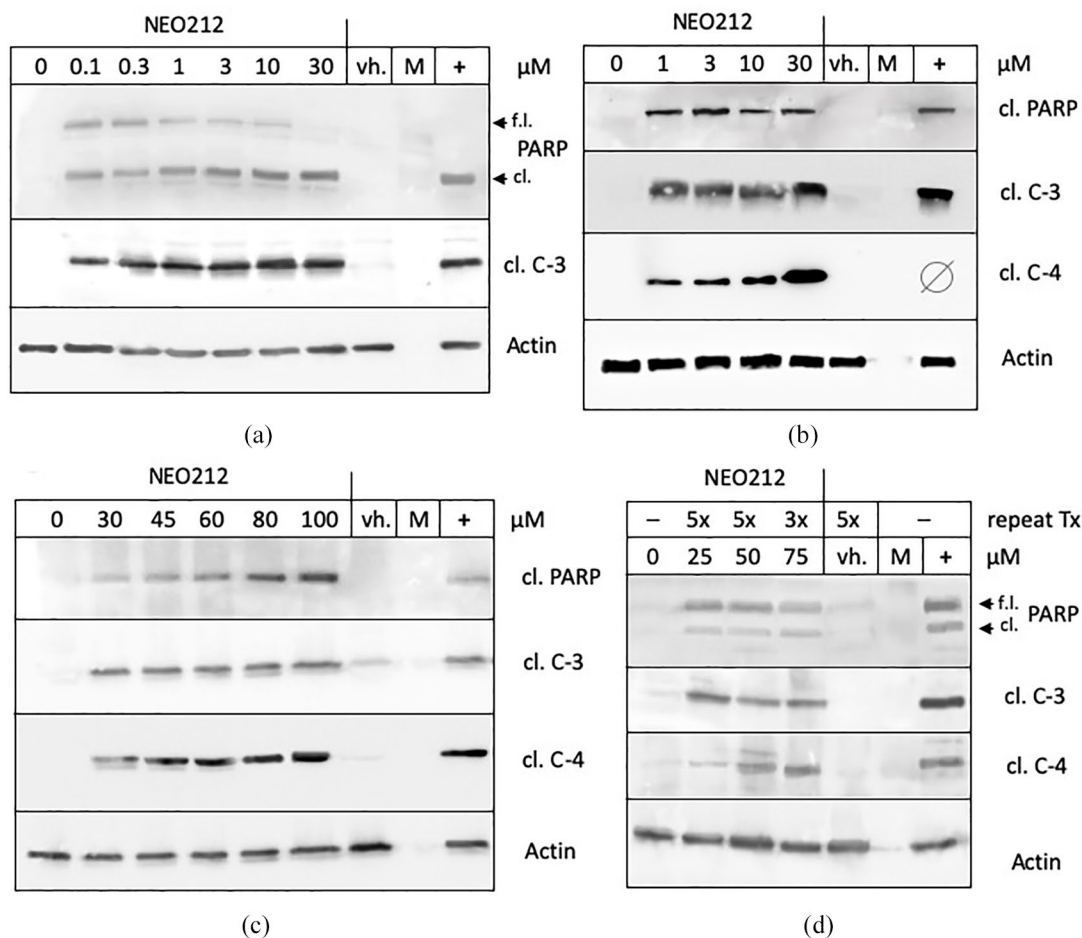
Figure 6. NEO212 induces protein markers of apoptosis.
HUT-78 cells (a), HUT-102 cells (b), and MyLa cells (c) were treated with increasing concentrations of NEO212 or vehicle (vh.). (a) and (b) were treated for 72h, and (c) for 96h. (d) MyLa cells received repeated treatments of NEO212: 25 and 50 μM NEO212 were added once per day for 5 consecutive days (5×), whereas 75 μM NEO212 was added once per day for 3 consecutive days (3×). Vehicle (vh.) was added once per day for 5 consecutive days (5×). Cells were harvested 24h after the final addition of NEO212 (or vehicle). In all cases, total cell lysates were prepared and subjected to Western blot analysis with specific antibodies to markers of cell death, including activated (i.e. cleaved, cl.) caspases, and PARP-1. For the latter, arrows point to its full-length (f.l.) and cl. form. Actin was used as the loading control. C-3, C-4: caspase 3 and caspase 4, respectively. M denotes a lane with molecular weight marker and '+' marks a lane with a positive control for the respective target antigen.

We next investigated established markers of apoptosis, such as cleavage of PARP-1 protein and activation (i.e. cleavage) of caspases. All three CTCL cell lines were treated with increasing concentrations of NEO212, and apoptosis markers were investigated by Western blot analysis. Figure 6 shows that treatment with NEO212 resulted in the appearance of cleaved PARP and cleaved (i.e. activated) caspases 3 and 4. The effects were similar in all three CTCL cell lines, except that somewhat higher concentrations of NEO212 were required in MyLa cells to achieve this outcome. As these latter cells proved to be somewhat less sensitive to NEO212, we further exposed them to repeat daily treatments with NEO212, as would be more relevant for general clinical use in the future. We added 25 or 50 μM NEO212 (or vehicle only) once daily for 5 consecutive days, and cells were harvested 24h after the final addition of drug. We also added 75 μM NEO212 on a daily basis, but here we collected cells already after the third treatment, owing to obvious, very extensive cell death. As shown in Figure 6(d), repeat treatments also triggered these apoptosis markers, although there was no clear-cut concentration-dependent effect. At the time of harvest, all three repeat treatment conditions had caused extensive unhealthy appearances of these cell cultures (as noted by microscopic

inspection), thus we suspect that each condition already resulted in maximal toxic insult. In any case, results shown in Figure 6 demonstrate potent induction of apoptotic cell death by NEO212 in all three CTCL cell lines.
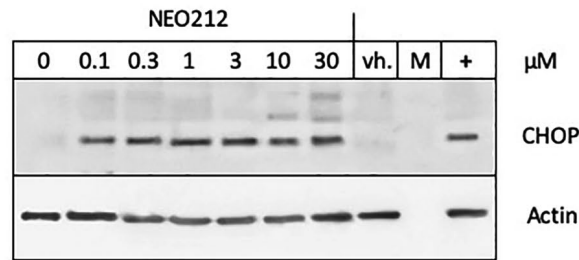
NEO212 induces endoplasmic reticulum stress and cell cycle arrest

To gain preliminary insight into mechanisms that might be involved in NEO212-induced apoptosis, we elucidated markers representing three different key processes governing cell fate. The first indicator was CHOP, a central component of the endoplasmic reticulum (ER) stress response that switches the dual mechanism of this response from its pro-survival to its pro-apoptosis mode.[30] The second indicator was the protein product of the c-myc proto-oncogene, a mitogenic transcription factor that often is overly active in cancer cells.[31] The third indicator was cyclin D1, a crucial cell cycle regulatory component that controls entry into S phase.[32]

Treatment with NEO212 resulted in prominent induction of CHOP protein in all three CTCL cell lines, indicating the presence of ER stress. Intriguingly, the lowest NEO212 concentrations applied to HUT78 and HUT102 cells, $0.1\,\mu M$ and $1.0\,\mu M$, respectively, sufficed to trigger near-maximal induction of this ER stress indicator (Figure 7(a) and (b)), whereas in MyLa cells CHOP induction was substantially more concentration dependent, with a gradual increase all the way up to $100\,\mu M$ NEO212 (Figure 7(c)). Conversely, expression levels of c-myc and cyclin D proteins declined in response to NEO212 treatment of HUT102 and MyLa cells (HUT78 cells were not tested). Together, these results reveal the emergence of pro-apoptotic ER stress in NEO212-treated cells, along with downregulation of a key mitogenic transcriptional stimulator, and inhibition of a component that is required for cell cycle progression. In concert, these events may provide a basis for the observed growth inhibition and apoptosis of NEO212-treated cells.

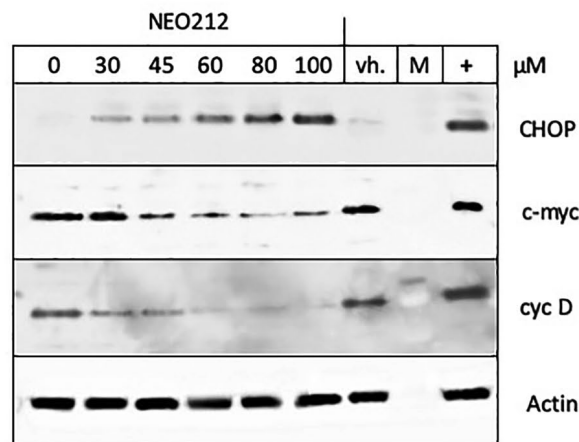### NEO212 effects are dependent on ROS production

The generation of reactive oxygen species (ROS) plays a role in chemotherapy of several anticancer drugs.[33] We therefore investigated whether ROS

(a)
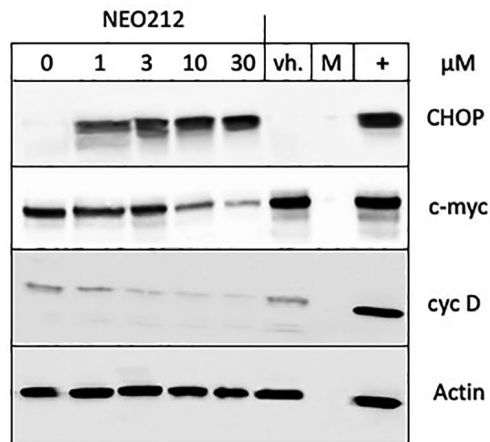
(b)

(c)

Figure 7. NEO212 induces protein markers of endoplasmic reticulum (ER) stress and inhibits cell proliferation markers.
HUT-78 cells (a), HUT-102 cells (b), and MyLa cells (c) were treated with increasing concentrations of NEO212 or vehicle (vh.). (a) and (b) were treated for 72 h, and (c) for 96 h. In all cases, total cell lysates were prepared and subjected to Western blot analysis with specific antibodies to markers of ER stress (CHOP) and cell proliferation (c-myc and cyclin D). Actin was used as the loading control. M denotes a lane with molecular weight marker and '+' marks a lane with a positive control for the respective target antigen.
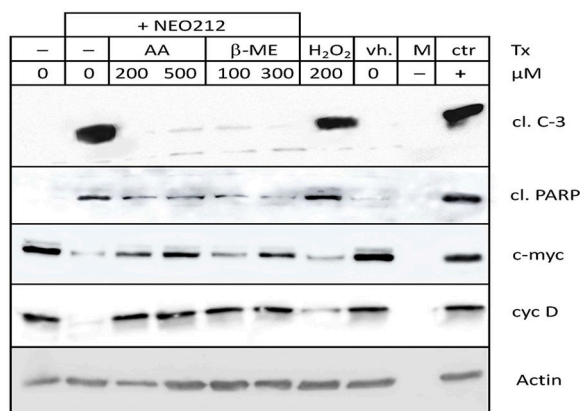
Figure 8. NEO212-mediated effects involve reactive oxidants.
MyLa cells received 200 and 500 μM AA or 100 and 300 μM β-ME, followed 15 min later by the addition of 80 μM NEO212. In parallel, cells were treated with 200 μM H_2O_2. After 48 hours, cells were harvested and lysates were analyzed by Western blot with specific antibodies. M denotes a lane with molecular weight marker and "+" marks a lane with a positive control for the respective target antigen. cl. C-3: cleaved (i.e. activated) caspase 3; cl. PARP: cleaved PARP-1.

might be involved in the above-described effects of NEO212, by including two commonly used antioxidants, ascorbic acid (AA) and beta-mercaptoethanol (β-ME).[34,35] MyLa cells were treated with NEO212 in the presence or absence of AA or β-ME, followed by analysis of the expression levels of c-myc and cyclin D1 (proliferation markers), and activated caspase-3 and cleaved PARP-1 (apoptosis markers). Figure 8 shows that AA and β-ME exerted striking effects, in that both agents prevented the anticancer effect of NEO212 on the selected marker proteins. In the presence of antioxidants, NEO212's prominent activation of caspase-3 was effectively blocked, and cleavage of PARP-1 was significantly diminished. Conversely, down-regulation of c-myc and cyclin D1 by NEO212 was prevented.

These results indicated that the growth-inhibitory and pro-apoptotic effects of NEO212 in these cells were largely mediated by drug-induced generation of ROS. To lend further support to this notion, we also treated cells with H_2O_2, to determine whether NEO212 effects on these same markers as above could be mimicked by directly supplying cells with ROS. As shown in Figure 8, this was indeed the case, as treatment of cells with H_2O_2 resulted in clear down-regulation of c-myc and cyclin D1 proteins, along with strong activation of caspase-3 and cleavage of PARP-1.

Discussion

MF and SS are complex diseases and difficult to manage. Physicians usually have to resort to the use of multiple therapies, and the situation becomes even more challenging in patients with advanced disease.[1,3] During early stages, skin-directed therapies, such as high-potency topical steroids, topical retinoids and rexinoids, topical nitrogen mustard, and phototherapy, represent first-line regimens with complete response rates ranging from 60% to 100%.[9,14,15] For patients at early stages who failed topical therapies, physicians can start using combinations with biologic agents, such as interferon alfa, retinoids (all-trans retinoic acid, isotretinoin), rexinoids (bexarotene), and methotrexate. Local radiation therapy is considered in patients with unifocal transformation, isolated/localized cutaneous tumors, or chronic and/or painful and/or ulcerated lesions. Extensive radiation therapies, such as total skin electron beam therapy (TSEBT), is generally reserved for elderly patients or patients with rapidly progressing or refractory widespread plaques and tumors.[4] At advanced stages of the disease, systemic therapy becomes necessary, but there is no standard regimen for these patients. A variety of approved and unapproved agents are used in these cases, including immune modulators and antibodies as single agents or as combination chemotherapy, or other investigational agents. The current US Food and Drug Administration (FDA)-approved agents for the treatment of CTCL are bexarotene, vorinostat, denileukin diftitox (discontinued in the United States), romidepsin, brentuximab vedotin, and mogamulizumab.[36] Despite these options, the need for additional and more effective therapeutic agents remains.

A few prior reports provided evidence that alkylating agents provided some benefit for patients with MF or SS. For example, topical carmustine [bis-chloroethylnitrosourea (BCNU)] has been used for patch- and plaque-stage MF.[37] Oral TMZ has been investigated in two phase II clinical trials with heavily pretreated, advanced-stage CTCL patients. The response rate was 33%[38] and 27%,[39] revealing moderate activity that compared favorably with other treatments. TMZ was also tested in four MF patients with central nervous system involvement, where it showed moderate activity as well.[40] These results inspired us to investigate NEO212 in MF/SS. Our prior studies with NEO212 established its potent anticancer activity, along with low toxicity, in a variety of

preclinical tumor models.[16–19] Although NEO212's therapeutic activity is at least in part based on DNA alkylation (derived from its TMZ component), the covalent conjugation to POH appears provide additional benefits, altogether resulting in significantly greater activity as compared with TMZ.[18] We therefore hypothesized that the promising, but moderate, activity of TMZ in MF/SS, as documented in three clinical studies, can be improved significantly with the use of NEO212.

When compared side-by-side *in vitro*, NEO212 exerted greater cytotoxic potency than TMZ in all three CTCL cell lines tested (Figure 3). Two of these cell lines (HUT78 and MyLa) essentially were unresponsive to TMZ, as IC50 was not reached at concentrations up to 300 µM. To put these numbers into a physiological context: peak plasma levels of TMZ in cancer patients have been measured in the range of 50–70 µM.[41,42] In comparison, HUT78 cells turned out to be exquisitely sensitive to NEO212, with concentrations as low as 1 µM NEO212 exerting significant ($p < 0.01$) growth-inhibitory effects (Figure 2), thus revealing a potency that was over 100-fold greater than that of TMZ (Figures 3 and 5). The particularly strong effects of NEO212 in HUT78 cells were the more impressive because these cells showed prominent expression of MGMT (Figure 4). MGMT is well known to confer powerful resistance to TMZ,[25,26] and unsurprisingly the two MGMT-positive cell lines, HUT78 and MyLa, were unresponsive to TMZ. Yet NEO212 did not follow this pattern: although effective in all three cell lines, its greatest potency was exerted in an MGMT-positive cell line. Altogether, these *in vitro* results indicate that NEO212 might overcome some of the therapeutic limitations of TMZ, in particular TMZ's ineffectiveness in patients with MGMT-positive tumors, which is well established in the case of malignant glioma.[43–45]

It is noteworthy that a mere mix of TMZ and POH at equimolar concentrations was unable to mimic the high potency of NEO212 in HUT78 or MyLa cells (Figure 3). There are a number of studies that have established the anticancer potential of POH in a variety of preclinical studies (see detailed references in Chen *et al.*[21]). In all cases, fairly high concentrations of this natural monoterpene, usually in the high micromolar to low millimolar range, were required to exert growth-inhibitory or apoptosis-inducing effects in cell culture. For example, several studies with GBM, breast cancer, or melanoma cell lines reported IC50s of 700–1800 µM of POH in various *in vitro* cytotoxicity assays.[16,17,46] Consistent with these earlier reports, our treatments with up to 300 µM POH show only negligible measurable impact on the three CTCL cell lines used (Figure 3). Accordingly, at concentrations up to 100 µM, the addition of POH to TMZ was unable to further enhance the cytotoxic effect over that of TMZ alone. For example, in HUT78 cells 100 µM TMZ alone reduced viability by about 30%, and treatment of cells with 100 µM TMZ in combination with 100 µM POH did not significantly further enhance this inhibitory effect. In comparison, 10 µM NEO212 reduced viability by over 50% (Figure 3(a)). This example illustrates that NEO212's potency is greater than the sum of its parts.

It is not entirely clear why covalent conjugation of TMZ to POH, as in NEO212, yields anticancer outcomes that are significantly greater than a mere mix of these two components. It is noteworthy that the cytotoxic effect of NEO212 treatment can be detected earlier than that of TMZ. The alkylating function of TMZ, in particular its methylation of the O6-position of guanine, generally requires two rounds of cell cycle progression to generate double-strand DNA breaks and subsequent cytotoxicity.[26,47] In contrast, cell growth-inhibitory effects of NEO212 can be detected within the first 24 h (Figure 2), which is more similar to the rapid cytotoxic effect of POH (although substantially higher concentrations of POH are required, as discussed above). These observations suggest that the inherent anticancer activity of NEO212 appears to involve more than DNA alkylation and that possibly POH-based activities are enhanced within its context of the NEO212 molecule.

Among the antitumor functions of POH is its ability to trigger cytotoxic ER stress, which has been demonstrated in GBM cells *in vitro*.[46] In general, the cellular ER stress response represents an adaptive mechanism by which the cell attempts to adjust to arising detrimental conditions, such as hypoxia, low nutrient levels, or certain pharmacological agents.[48] However, if homeostasis cannot be re-established, the pro-apoptotic module of this mechanism, in particular its key executor protein CHOP, gains dominance and tips the balance toward cell death.[30] Our finding that NEO212 treatment of CTCL cells results in pronounced CHOP induction (Figure 7) suggests

that ER stress might play a role in NEO212-induced cell death. This view is supported further by the observed decline in cyclin D protein levels (Figure 7). As it has been established[49] that ER stress results in down-regulation of this cell cycle regulator, our results are consistent with a role for ER stress. As well, NEO212 treatment resulted in the down-regulation of c-myc protein, which is noteworthy in view of this proto-oncoprotein's central role in cell proliferation and oncogenesis.[31] Although not generally controlled by ER stress, there is an example in the literature where treatment of mouse or rat pre-adipocytes with palmitate resulted in aggravated ER stress (i.e. CHOP induction), along with down-regulation of c-myc (and cyclin D), followed by cellular apoptosis.[50] Altogether, these considerations point to the possibility that the ER stress-aggravating function of POH is preserved in the NEO212 molecule and possibly enhanced within the context of the chimeric construct.

In any case, NEO212-induced death of CTCL cells appears to be executed primarily *via* apoptosis. Proteolytic cleavage of caspases and PARP-1 protein, resulting in activation of caspases and inactivation of PARP-1, represents a well-established and widely used marker of apoptotic cell death.[51,52] In both HUT78 and HUT102 cells, NEO212 triggered the emergence of these markers at very low concentrations ($0.1–1.0\,\mu M$). In MyLa cells, the same effect was observed, although higher ($30\,\mu M$) NEO212 concentrations were required (Figure 6). Of note, the inclusion of commonly used antioxidants, that is, ascorbic acid and beta-mercaptoethanol,[34,35] largely prevented the induction of these apoptotic markers, suggesting that ROS might play a key role in mediating the cell death-inducing effects of NEO212. This model is consistent with our observation that direct addition of ROS to the cells, in the form of hydrogen peroxide, mimicked NEO212's effect on markers of apoptosis and proliferation (Figure 8), and is further supported by earlier studies of NEO212 in human nasopharyngeal carcinoma and non-small cell lung cancer cells, which showed that NEO212 was able to trigger ROS accumulation in these cancer types *in vitro*.[53–55] It therefore appears that NEO212's anticancer mechanism is at least in part similar to what has been reported for some of the well-established chemotherapeutic agents, such as doxorubicin and cisplatin, where the accumulation of ROS has been shown to further enhance their DNA-damaging and apoptosis-inducing potential.[53,56]

In summary, we present data demonstrating the high anticancer potency of NEO212 in CTCL cell lines. Compared with both of its individual components, TMZ and POH, NEO212 exerts substantially greater cytotoxic activity, potentially *via* involvement of the pro-apoptotic module of the ER stress response mechanism, although its alkylating activity might contribute as well. As a next step in NEO212's development, *in vivo* experiments in immunodeficient murine CTCL models should be performed. We have attempted such models, but tumor take with our CTCL cell lines was unacceptably low, not inconsistent with reported challenges of achieving consistent tumor growth with these and other CTCL cell lines in general.[57–59] It is conceivable that serial passage of positive tumors in mice would yield more aggressive cells, and we are considering pursuing this approach. In addition, we have performed toxicity studies in mice (see Supplemental Data in Chen *et al.*[16,17]) and Beagle dogs (unpublished) and determined that NEO212 is very well tolerated, which bodes well for future clinical studies.

Conflict of interest statement
TCC is founder and stakeholder of NeOnc Technologies, Los Angeles, CA. No potential conflict of interest was disclosed by the other authors.

ORCID iD
Axel H. Schönthal [iD] https://orcid.org/0000-0003-0662-5653

References
1. Wilcox RA. Cutaneous T-cell lymphoma: 2016 update on diagnosis, risk-stratification, and management. *Am J Hematol* 2016; 91: 151–165.

2. McGirt LY, Jia P, Baerenwald DA, *et al.* Whole-genome sequencing reveals oncogenic mutations in mycosis fungoides. *Blood* 2015; 126: 508–519.

3. Trautinger F, Eder J, Assaf C, *et al.* European Organisation for Research and Treatment of Cancer consensus recommendations for the treatment of mycosis fungoides/Sézary syndrome - update 2017. *Eur J Cancer* 2017; 77: 57–74.

4. Jawed SI, Myskowski PL, Horwitz S, *et al.* Primary cutaneous T-cell lymphoma (mycosis fungoides and Sézary syndrome): part I. Diagnosis: clinical and histopathologic features and new molecular and biologic markers. *J Am Acad Dermatol* 2014; 70: 205 e201–e216; quiz 221–202.

5. Korgavkar K, Xiong M and Weinstock M. Changing incidence trends of cutaneous T-cell lymphoma. *JAMA Dermatol* 2013; 149: 1295–1299.

6. Wilson LD, Hinds GA and Yu JB. Age, race, sex, stage, and incidence of cutaneous lymphoma. *Clin Lymphoma Myeloma Leuk* 2012; 12: 291–296.

7. Ringrose A, Zhou Y, Pang E, *et al.* Evidence for an oncogenic role of AHI-1 in sézary syndrome, a leukemic variant of human cutaneous T-cell lymphomas. *Leukemia* 2006; 20: 1593–1601.

8. Willemze R. Mycosis fungoides variants-clinicopathologic features, differential diagnosis, and treatment. *Semin Cutan Med Surg* 2018; 37: 11–17.

9. Spicknall KE. Sezary syndrome-clinical and histopathologic features, differential diagnosis, and treatment. *Semin Cutan Med Surg* 2018; 37: 18–23.

10. Girardi M, Heald PW and Wilson LD. The pathogenesis of mycosis fungoides. *N Engl J Med* 2004; 350: 1978–1988.

11. Prince HM and Querfeld C. Integrating novel systemic therapies for the treatment of mycosis fungoides and Sézary syndrome. *Best Pract Res Clin Haematol* 2018; 31: 322–335.

12. Swerdlow SH, Campo E, Pileri SA, *et al.* The 2016 revision of the World Health Organization classification of lymphoid neoplasms. *Blood* 2016; 127: 2375–2390.

13. da Silva Almeida AC, Abate F, Khiabanian H, *et al.* The mutational landscape of cutaneous T cell lymphoma and Sézary syndrome. *Nat Genet* 2015; 47: 1465–1470.

14. Querfeld C, Zain J and Rosen ST. Primary cutaneous T-cell lymphomas: mycosis fungoides and sezary syndrome. *Cancer Treat Res* 2019; 176: 225–248.

15. Larocca C and Kupper T. Mycosis fungoides and Sézary syndrome: an update. *Hematol Oncol Clin North Am* 2019; 33: 103–120.

16. Chen TC, Cho HY, Wang W, *et al.* A novel temozolomide-perillyl alcohol conjugate exhibits superior activity against breast cancer cells in vitro and intracranial triple-negative tumor growth in vivo. *Mol Cancer Ther* 2014; 13: 1181–1193.

17. Chen TC, Cho HY, Wang W, *et al.* A novel temozolomide analog, NEO212, with enhanced activity against MGMT-positive melanoma in vitro and in vivo. *Cancer Lett* 2015; 358: 144–151.

18. Chen TC, Da Fonseca CO and Schönthal AH. Perillyl alcohol and its drug-conjugated derivatives as potential novel methods of treating brain metastases. *Int J Mol Sci* 2016; 17: 1463.

19. Jhaveri N, Agasse F, Armstrong D, *et al.* A novel drug conjugate targeting proneural and mesenchymal subtypes of patient-derived glioma cancer stem cells. *Cancer Lett*. Epub ahead of print 9 December 2015. DOI: 10.1016/j.canlet.2015.11.040.

20. Crowell PL and Elson CE. Isoprenoids, health and disease. In: Wildman REC (ed) *Neutraceuticals and functional foods*. Boca Raton, FL: CRC Press, 2001.

21. Chen TC, Fonseca CO and Schönthal AH. Preclinical development and clinical use of perillyl alcohol for chemoprevention and cancer therapy. *Am J Cancer Res* 2015; 5: 1580–1593.

22. Chen TC, da Fonseca CO and Schonthal AH. Intranasal perillyl alcohol for glioma therapy: molecular mechanisms and clinical development. *Int J Mol Sci* 2018; 19: 3905.

23. Chua J, Nafziger E and Leung D. Evidence-based practice: temozolomide beyond glioblastoma. *Curr Oncol Rep* 2019; 21: 30.

24. Teimouri F, Nikfar S and Abdollahi M. Efficacy and side effects of dacarbazine in comparison with temozolomide in the treatment of malignant melanoma: a meta-analysis consisting of 1314 patients. *Melanoma Res* 2013; 23: 381–389.

25. Lee SY. Temozolomide resistance in glioblastoma multiforme. *Genes Dis* 2016; 3: 198–210.

26. Roos WP and Kaina B. DNA damage-induced cell death: from specific DNA lesions to the DNA damage response and apoptosis. *Cancer Lett* 2013; 332: 237–248.

27. Kim SR, Lewis JM, Cyrenne BM, *et al.* BET inhibition in advanced cutaneous T cell lymphoma is synergistically potentiated by BCL2

inhibition or HDAC inhibition. *Oncotarget* 2018; 9: 29193–29207.

28. Harlow E and Lane D. *Using antibodies: a laboratory manual.* Cold Spring Harbor, NY: Cold Spring Harbor Laboratory, 1999.

29. Omura S, Asami Y and Crump A. Staurosporine: new lease of life for parent compound of today's novel and highly successful anti-cancer drugs. *J Antibiot (Tokyo)* 2018; 71: 688–701.

30. Li Y, Guo Y, Tang J, *et al.* New insights into the roles of CHOP-induced apoptosis in ER stress. *Acta Biochim Biophys Sin (Shanghai)* 2014; 46: 629–640.

31. Carroll PA, Freie BW, Mathsyaraja H, *et al.* The MYC transcription factor network: balancing metabolism, proliferation and oncogenesis. *Front Med* 2018; 12: 412–425.

32. Musgrove EA, Caldon CE, Barraclough J, *et al.* Cyclin D as a therapeutic target in cancer. *Nat Rev Cancer* 2011; 11: 558–572.

33. Srinivas US, Tan BWQ, Vellayappan BA, *et al.* ROS and the DNA damage response in cancer. *Redox Biol* 2018: 101084.

34. Buettner GR. The pecking order of free radicals and antioxidants: lipid peroxidation, alpha-tocopherol, and ascorbate. *Arch Biochem Biophys* 1993; 300: 535–543.

35. Knight JA. Review: free radicals, antioxidants, and the immune system. *Ann Clin Lab Sci* 2000; 30: 145–158.

36. Alpdogan O, Kartan S, Johnson W, *et al.* Systemic therapy of cutaneous T-cell lymphoma (CTCL). *Chin Clin Oncol* 2019; 8: 10.

37. Zackheim HS. Topical carmustine (BCNU) in the treatment of mycosis fungoides. *Dermatol Ther* 2003; 16: 299–302.

38. Tani M, Fina M, Alinari L, *et al.* Phase II trial of temozolomide in patients with pretreated cutaneous T-cell lymphoma. *Haematologica* 2005; 90: 1283–1284.

39. Querfeld C, Rosen ST, Guitart J, *et al.* Multicenter phase II trial of temozolomide in mycosis fungoides/sézary syndrome: correlation with O^6-methylguanine-DNA methyltransferase and mismatch repair proteins. *Clin Cancer Res* 2011; 17: 5748–5754.

40. Bird TG, Whittaker S, Wain EM, *et al.* Temozolomide for central nervous system involvement in mycosis fungoides. *Int J Dermatol* 2016; 55: 751–756.

41. Brada M, Judson I, Beale P, *et al.* Phase I dose-escalation and pharmacokinetic study of temozolomide (SCH 52365) for refractory or relapsing malignancies. *Br J Cancer* 1999; 81: 1022–1030.

42. Hammond LA, Eckardt JR, Baker SD, *et al.* Phase I and pharmacokinetic study of temozolomide on a daily-for-5-days schedule in patients with advanced solid malignancies. *J Clin Oncol* 1999; 17: 2604–2613.

43. Chamberlain MC. Temozolomide: therapeutic limitations in the treatment of adult high-grade gliomas. *Expert Rev Neurother* 2010; 10: 1537–1544.

44. Hegi ME, Diserens AC, Gorlia T, *et al.* MGMT gene silencing and benefit from temozolomide in glioblastoma. *N Engl J Med* 2005; 352: 997–1003.

45. Kaina B and Christmann M. DNA repair in personalized brain cancer therapy with temozolomide and nitrosoureas. *DNA Repair (Amst)* 2019; 78: 128–141.

46. Cho HY, Wang W, Jhaveri N, *et al.* Perillyl alcohol for the treatment of temozolomide-resistant gliomas. *Mol Cancer Ther* 2012; 11: 2462–2472.

47. Knizhnik AV, Roos WP, Nikolova T, *et al.* Survival and death strategies in glioma cells: autophagy, senescence and apoptosis triggered by a single type of temozolomide-induced DNA damage. *PLoS One* 2013; 8: e55665.

48. Schönthal AH. Pharmacological targeting of endoplasmic reticulum stress signaling in cancer. *Biochem Pharmacol* 2013; 85: 653–666.

49. Brewer JW, Hendershot LM, Sherr CJ, *et al.* Mammalian unfolded protein response inhibits cyclin D1 translation and cell-cycle progression. *Proc Natl Acad Sci U S A* 1999; 96: 8505–8510.

50. Guo W, Wong S, Xie W, *et al.* Palmitate modulates intracellular signaling, induces endoplasmic reticulum stress, and causes apoptosis in mouse 3T3-L1 and rat primary preadipocytes. *Am J Physiol Endocrinol Metab* 2007; 293: E576–E586.

51. Soldani C and Scovassi AI. Poly(ADP-ribose) polymerase-1 cleavage during apoptosis: an update. *Apoptosis* 2002; 7: 321–328.

52. Li J and Yuan J. Caspases in apoptosis and beyond. *Oncogene* 2008; 27: 6194–6206.

53. Marullo R, Werner E, Degtyareva N, *et al.* Cisplatin induces a mitochondrial-ROS response that contributes to cytotoxicity depending on mitochondrial redox status and bioenergetic functions. *PLoS One* 2013; 8: e81162.

54. Song X, Xie L, Wang X, *et al.* Temozolomide-perillyl alcohol conjugate induced reactive oxygen species accumulation contributes to its cytotoxicity against non-small cell lung cancer. *Sci Rep* 2016; 6: 22762.

55. Xie L, Song X, Guo W, *et al.* Therapeutic effect of TMZ-POH on human nasopharyngeal carcinoma depends on reactive oxygen species accumulation. *Oncotarget* 2016; 7: 1651–1662.

56. Conklin KA. Chemotherapy-associated oxidative stress: impact on chemotherapeutic effectiveness. *Integr Cancer Ther* 2004; 3: 294–300.

57. Netchiporouk E, Gantchev J, Tsang M, *et al.* Analysis of CTCL cell lines reveals important differences between mycosis fungoides/Sézary syndrome vs. *HTLV-1*+ leukemic cell lines. *Oncotarget* 2017; 8: 95981–95998.

58. Doebbeling U. A mouse model for the Sézary syndrome. *J Exp Clin Cancer Res* 2010; 29: 11.

59. Thaler S, Burger AM, Schulz T, *et al.* Establishment of a mouse xenograft model for mycosis fungoides. *Exp Dermatol* 2004; 13: 406–412.

Visit SAGE journals online
journals.sagepub.com/
home/tam

SAGE journals